

# Deterministic and Stochastic Optimal Control for Batch Cooling Crystallization

Tushar Gupta

---

## Abstract

This paper presents a stochastic model predictive control (MPC) approach for non-linear systems which involve time-invariant probabilistic uncertainties in their model parameters. The field in focus here is batch crystallization which is affected heavily by the errors or uncertainties that creep into the model during real world applications and result in sub-par performance when compared to in-house simulations. Uncertainty quantification helps to mitigate this problem by incorporating the errors, in the optimization algorithms while performing predictive control. Each of the optimization algorithms entail a cost function which maximises the amount or the expected value of the desired product. First, this work presents a deterministic study to highlight the kinetics of the batch process and then draws comparison with the stochastic process to indicate an increase in performance in the later. The dynamic uncertainties in the process are modelled using Ito's lemma, stochastic calculus and stochastic maximum principle. In the end, a novel approach named Polynomial Chaos Expansions is implemented for the control strategy, which has been applied successfully to other domains for non-linear MPC but was not explored in detail in the field of batch cooled crystallization. It successfully includes probability distributions for the parameters into the model to provide a more robust optimization strategy.

**Keywords:** Stochastic Optimal Control, Polynomial Chaos Expansions, Robust Optimization, Batch Crystallization, Predictive Control, Optimum Temperature Profile

---

## 1. Introduction

Numerous industries today, such as pharmaceutical, chemical, photographic etc. employ the batch crystallization process for the preparation of crystalline products with high degree of purity. A common goal of each crystallization process is to obtain a narrower Particle size distribution (PSD) of the desired product. The PSD has a strong influence on the downstream processing and, hence, reproducible PSD in each operation is of prime importance. Thus, finding an effective control strategy to obtain the resulting crystals with a desired Crystal Size Distribution becomes significant in order for improving the performance of both the batch crystallization process and the subsequent processes which depend on it.

Crystallization is the (natural or artificial) process where the atoms or molecules are highly organized into a solid structure known as a crystal. Some of the ways which crystals form are through precipitating from a solution, melt or more rarely deposited directly from a gas. In order for crystallization to take place a solution must be "super-saturated". **Supersaturation**( $\Delta C$ ) is a condition in which the solute concentration in the solution is higher than the solubility. It acts as the driving force for the crystallization process and affects the final quantity of product formed. It is mathematically expressed as :

$$\Delta C = C - C_s \quad (1)$$

where  $C_s$  is the concentration of the solute in the saturated solution. In the following work, the method in focus is cooling crystallization in which superstauration magnitude is determined by the cooling rate. Thus, determination of an optimal cooling rate or a temperature trajectory becomes the objective of the current study.

This work formulates and analyses various control strategies for a cooling crystallization process represented through the population balance equation. **Deterministic Optimal Control** aims at finding the an optimum temperature profile to maximise an objective function selected to achieve a desired volume of the product. Herein, the experimental kinetic parameters are employed to simulate a batch crystallization process. **Stochastic Optimal Control** undertakes the task of quantifying the uncertainities which creep in due to experimentation. It aims to achieve a maximum expected value for the desired product, simultaneously incorporating randomness in the process parameters into the model. Namely, two methods **Ito Process** and a novel approach **Polynomial Chaos Expansions** are employed for this purpose.

Most of the reported works in the this field deal with the determination of optimal temperature or supersaturation trajectory for the batch crystallizer. The concept of programmed cooling in batch crystallizers was first discussed by Mullin and Nývlt (1971). Later, Jones (1974) presented a mathematical theory based on moment transformations of population balance equations. He used the continuous maximum principle to predict optimal cooling curves. Rawlings et al. (1992) discussed issues in crystal size measurement using laser light scattering experiments and optimal control problem formulation. Miller and Rawlings (1994) discussed the uncertain bounds on model parameter estimates for a batch crystallization system. Most importantly optimal temperature prediction for batch crystallization has also been done by Hu et al. (2005), Shi et al. (2006), Paengjuntuek et al. (2008) and Corriou and Rohani (2008), the data and knowledge from which have been used in further work in this project.

Stochastic modeling of particulate processes and parameter estimation using the experimentally measured particle sizes has attracted many researchers. Grosso et al. (2011) presented a stochastic approach for modeling PSD and comparative assessments of different models. Ma et al. (1999) presented a worse-case performance analysis of optimal control trajectories by considering features such as the computational effort, parametric uncertainty and control implementation inaccuracies. Monte Carlo simulations have also been used to propogate uncertainties but often present the problem of high computational demand, for which this work proposes Polynomial Chaos Expansions(PCEs) as an alternative. The computational advantages of PCEs for robust control and optimization has been shown by Nagy and Braatz (2007), Kim and Braatz (2012) and Kumar and Budman (2014).

The focus of the current research activity is to incorporate parametric uncertainties in the mathematical formulations of batch crystallization process for building a robust model. In the deterministic approach, kinetic parameters from the experimental data have been used to model the system. Next, stochastic Ito processes are used to assimilate the errors in the experimental data. Finally, PCE are demonstrated as an effective method for non-linear optimization in batch reactors. A case study of an unseeded crystallization process is also included to authenticate the methodology.

## 2. Materials and methods

This section introduces the underlying concepts needed to build a computational model of a crystallization process which involves regulating the population of particles, also termed as a particulate process. The population is described by the density of a suitable extensive variable, usually the **number of particles**, but sometimes by other variables such as the mass or volume of particles. The usual transport equations expressing conservation laws for material systems apply to the behavior of single particles. Particulate processes are characterized by properties such as particle shape, size, surface area, mass, and product purity.

A population balance formulation describes the process of crystal size distribution with time most effectively. Thus, modeling of a batch crystallizer involves the use of population balances to model the crystal size prediction and the mass balance on the system can be modeled as a simple differential equation having concentration as the state variable. The population balance can be expressed as follows :

$$\frac{\partial n(r, t)}{\partial t} + \frac{\partial G(r, t)n(r, t)}{\partial r} = B \quad (2)$$

where **n** is the number density distribution, **t** is the time, **r** represents the characteristic dimension for size measurements, **G** is the crystal growth rate, and **B** is the nucleation rate. Both growth and nucleation processes describe crystallization kinetics, and their expression may vary, depending on the system under consideration.

In this work, the system under consideration is potassium sulfate, which has been studied earlier for its kinetics by Hu et al. (2005), Shi et al. (2006) and Paengjuntuek et al. (2008). The equations expressing the kinetics and values for the kinetic parameters have been derived form these literary works.

Nucleation kinetics are defined by :

$$B(t) = k_b \exp(-E_b/RT) \left( \frac{C - C_s(T)}{C_s(T)} \right)^b \mu_3 \quad (3)$$

Growth Kinetics are given by:

$$G(t) = k_g \exp(-E_g/RT) \left( \frac{C - C_s(T)}{C_s(T)} \right)^g \quad (4)$$

where  $k_b$  and  $k_g$  are constants of the system,  $E_b$  and  $E_g$  are activation energies, and  $b$  and  $g$  are exponents of nucleation and growth, respectively. The values for these parameters for the given system have been mentioned in Table 1. The following equations are used to evaluate the saturation( $C_s$ ) and metastable( $C_m$ ) concentrations corresponding to the solution temperature  $T$  (expressed in units of °C) (Shi et al. (2006)).

$$C_s(T) = 6.29 \times 10^{-2} + 2.46 \times 10^{-3}T - 7.14 \times 10^{-6}T^2 \quad (5)$$

$$C_m(T) = 7.76 \times 10^{-2} + 2.46 \times 10^{-3}T - 8.1 \times 10^{-6}T^2 \quad (6)$$

The mass balance, in terms of concentration of the solute in the solution, is expressed as :

$$\frac{dC}{dt} = -3\rho k_v G(t) \mu_2(t) \quad (7)$$

where  $\rho$  is the density of the crystals,  $k_v$  the volumetric shape factor, and  $\mu_2$  is the second moment of particle size distribution (PSD). Since  $n(r, t)$  represents the population density of the crystals, the  $i$ -th moment of the particle size distribution(PSD) is given by :

$$\mu_i = \int_0^\infty r^i n(r, t) dr \quad (8)$$

The above equations along with the Population Balance Equation(PBE) (2) represent a complete model of a seeded batch crystallizer. Population balance equations are multidimensional, which poses a problem with their implementation in complex control functions, hence use of a model order reduction becomes imperative.

For simplification, we reduce the population balance equations into **Moment balance equations** which has been established as an efficient method by Yenkie and Diwekar (2012). This is done by multiplying (2) with  $r^i$  on both sides to generate the expression given by (8). Converting the model into Ordinary differential equations proves to be advantageous, since it is difficult and time-consuming to formulate an optimization problem involving PBEs. Thus, the moment method leads to a reduced-order model given by Equations (11) to (14)

Separate moment equations are used for the seed and nuclei classes of crystals, and they are defined as :

$$\mu_i^n = \int_0^{r_g} r^i n(r, t) dr \quad (9)$$

$$\mu_i^s = \int_{r_g}^\infty r^i n(r, t) dr \quad (10)$$

$\mathbf{n}$  in the superscript represents the nucleated crystal whereas  $\mathbf{s}$  stands for the seeded crystal,  $r_g$  gives the critical radius separating the two. The resultant moment equations for nucleated and seeded crystals are as follows (Yenkie and Diwekar (2012)) :

#### 1. Nucleated crystals

$$\frac{d\mu_0^n}{dt} = B(t) \quad (11)$$

$$\frac{d\mu_i^n}{dt} = iG(t)\mu_{i-1}^n(t) \quad i = 1, 2, 3 \quad (12)$$

## 2. Seeded crystals

$$\mu_0^s = \text{constant} \quad (13)$$

$$\frac{d\mu_i^s}{dt} = iG(t)u_{i-1}^n(t) \quad i = 1, 2, 3 \quad (14)$$

The total moment is obtained as the summation  $\mu_i^t = \mu_i^n + \mu_i^s$ . Here,  $\mu_0^s$  represents the amount of seeded crystals and hence remains constant. Also, fourth-order moments and higher do not affect third-order moments and lower, implying that only the first four moments and concentration can adequately represent the crystallization dynamics (Shi et al. (2006)).

The crystallization model defined above has been used to compare the performance of different types of optimization techniques, both in the deterministic and stochastic domain, which is explained in detail in the subsequent sections.

Table 1. Experimental values of Kinetic Parameters

Parameters	Experimental Values
Growth Kinetics	
$k_g$	$1.44 \times 10^8 \mu\text{ms}^{-1}$
$E_g/R$	4859K
$g$	1.5
Nucleation Kinetics	
$k_b$	$285(s\mu\text{m}^3)^{-1}$
$E_b/R$	7517K
$b$	1.45

## 3. Deterministic Optimal Control

### 3.1. Seeded batch crystallization

Optimal control involves the evaluation of time-dependent operating profiles, in terms of the control variable to optimize the process performance. In the crystallization domain, temperature becomes the control variable while the product yield is used to evaluate the performance of the model. The Optimization problem here is solved by using the method of Maximum Principle as discussed extensively by Diwekar (2008). This method stands out in compared to other techniques such as dynamic programming as it involves the use of first order ODEs while the later utilises partial differential equations. Another advantage of maximum principle is its ability to adapt to stochastic calculus which is explained in the next section.

In a seeded crystallization process it is essential to keep the nucleation phenomena to minimum as in the early stages of growth, nucleated crystals might compete with the seeded ones for growth. This ensures uniformity in the shape and size of the final product. It is achieved by incorporating the volume of nucleated in the **objective function**. Third moment( $\mu_3$ ) represents volume in a crystallization model as evident from (8) and is used as follows :

$$\max_{T(t)} \{\mu_3^s(t_f) - \mu_3^n(t_f)\} \quad (15)$$

The active constraints for the process are given by :

$$C_s \leq C \leq C_m \quad (16)$$

$C_m$  is the metastable concentration described by (6). The state variables  $y_i$  for the process are now represented as :

$$y_i = \begin{bmatrix} C & \mu_0^s & \mu_1^s & \mu_2^s & \mu_3^s & \mu_0^n & \mu_1^n & \mu_2^n & \mu_3^n \end{bmatrix} \quad (17)$$

Using the above notations the state equations can be realized as (Yenkie and Diwekar (2012)) :

$$\frac{dy_1}{dt} = -3\rho k_v G(t)(y_4 + y_8) \quad (18)$$

$$\frac{dy_2}{dt} = 0 \quad (19)$$

$$\frac{dy_3}{dt} = G(t)y_2 \quad (20)$$

$$\frac{dy_4}{dt} = 2G(t)y_3 \quad (21)$$

$$\frac{dy_5}{dt} = 3G(t)y_4 \quad (22)$$

$$\frac{dy_6}{dt} = B(t) \quad (23)$$

$$\frac{dy_7}{dt} = G(t)y_6 \quad (24)$$

$$\frac{dy_8}{dt} = 2G(t)y_7 \quad (25)$$

$$\frac{dy_9}{dt} = 3G(t)y_8 \quad (26)$$

$$(27)$$

Thus, the complete model involving the moment equations consists of nine state equations.

### 3.2. Solution technique

The algorithm of Steepest Ascent utilizes the Maximum Principle using the Hamiltonian to move towards the optimum value of temperature and maximise the objective function. To formulate the equations an adjoint variable ( $z_i$ ) is defined corresponding to each state variable ( $y_i$ ). The adjoint variable satisfy the relations given by (31). Using the state and the adjoint equations, a two-point boundary-value-problem is constructed. Here, the initial values for the states and the final conditions for the adjoint variables are known beforehand. The Hamiltonian can now be defined by (28).

$$H = \sum_{i=1}^9 z_i f(y_i, t, T) \quad (28)$$

The complete model with the objective function is given by Equations (29) to (31):

$$\max_{T(t)} \{y_5(t_f) - y_9(t_f)\} \quad (29)$$

$$\frac{dy_i}{dt} = f(y_i, t, T) \quad (30)$$

$$\frac{dz_i}{dt} = \sum_{j=1}^9 z_j \frac{\partial f(y_j, t, T)}{\partial y_i} = f(y_i, z_i, t, T) \quad (31)$$

with the initial and final conditions:

$$\begin{aligned} t_0 &= 0 \quad \text{and} \quad t_f = 1800s \quad (\text{batch time}) \\ y_i(t_0) &= [0.1743 \quad 66.66 \quad 1.83 \times 10^4 \quad 5.05 \times 10^6 \quad 1.93 \times 10^9 \quad 0.867 \quad 0 \quad 0 \quad 0] \\ z_i(t_f) &= [0 \quad 0 \quad 0 \quad 0 \quad 1 \quad 0 \quad 0 \quad 0 \quad -1] \end{aligned}$$

The steps followed to solve the optimal control problem have been discussed in detail below.

1. An initial temperature  $T(t) = 323K$  is assumed for the entire time horizon.

2. The differential equations for state variables( $y_i$ ) are integrated in the forward direction using the given initial conditions.
3. The values of the adjoint variables( $z_i$ ) are computed by backward integration of the adjoint equations given by (31).
4. For evaluation of the Hamiltonian derivative, an analytical method proposed by Benavides and Diwekar (2012), is used in which an additional variable corresponding to each of the state and adjoint variable is introduced. The variable  $\theta_i$  corresponds to each of the state variable  $y_i$  and the variable  $\phi_i$  corresponds to each of the adjoint variable  $z_i$ , which is given by (32).

$$\theta_i = \frac{dy_i}{dT} \quad \text{and} \quad \phi_i = \frac{dz_i}{dT} \quad (32)$$

5. The variables  $\theta_i$  and  $\phi_i$  along with  $y_i$  and  $z_i$  give the derivative of Hamiltonian by (36). The differential equations used for computing  $\theta_i$  and  $\phi_i$  are obtained by the following method :

$$\frac{d\left(\frac{dy_i}{dT}\right)}{dT} = \frac{d\left(\frac{dy_i}{dT}\right)}{dt} = \frac{d\theta_i}{dt} \quad (33)$$

$$\frac{d\left(\frac{dz_i}{dT}\right)}{dT} = \frac{d\left(\frac{dz_i}{dT}\right)}{dt} = \frac{d\phi_i}{dt} \quad (34)$$

The initial conditions used for forward integration of  $\frac{d\theta_i}{dt}$  are  $\theta_i(t_0) = [0 \ 0 \ 0 \ 0 \ 0 \ 0 \ 0 \ 0 \ 0]$  and the final conditions used for the backward integration of  $\frac{d\phi_i}{dt}$  are  $\phi_i(t_f) = [0 \ 0 \ 0 \ 0 \ 0 \ 0 \ 0 \ 0 \ 0]$

6. The Hamiltonian derivative is now calculated at each time step by (36).

$$\frac{dH}{dT} = \sum_{i=1}^9 \left( \frac{dH}{dy_i} \right) \left( \frac{dy_i}{dT} \right) + \sum_{i=1}^9 \left( \frac{dH}{dz_i} \right) \left( \frac{dz_i}{dT} \right) \quad (35)$$

$$\frac{dH}{dT} = \sum_{i=1}^9 \left( \frac{dH}{dy_i} \right) \theta_i + \sum_{i=1}^9 \left( \frac{dH}{dz_i} \right) \phi_i \quad (36)$$

7. The computed value of the derivative is checked against the convergence criterion ( $\frac{dH}{dT} < \text{tolerance}$ ). If it is not satisfied, the temperature  $T(t)$  is updated using (37). This ensures that the optimal control variable  $T(t)$  is obtained using the extremum of Hamiltonian.

$$T^{new}(t) = T^{old}(t) + M \left( \frac{dH}{dT} \right) \quad (37)$$

8. The concentration is evaluated at that time step and compared with first with the saturation concentration ( $C_s$ ) and then the metastable concentration( $C_m$ ) to validate the active constraints. If it found to be lesser than saturation value or greater than the metastable value, (5) and (6) are used to compute the new temperature respectively.
9. Iterations of above steps are repeated until the convergence criteria is achieved.

### 3.3. Results

The integration of differential equations was performed in python using the odeint routine from the scipy open source package. The resultant optimal temperature profile is shown in Figure 1. The system attains a constant value of 300K at  $\sim 1700s$ . The decreasing temperature profile is indicative of the cooling crystallization. Also, the objective function can be observed to reach a maximum value in the Figure 2. The concentration profile of solute in the system is given by the Figure 3.

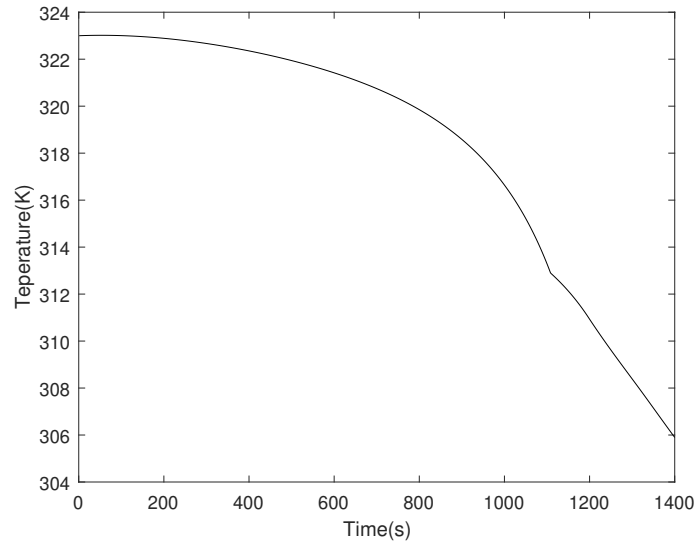


Figure 1. The optimal cooling profile  $T(t)$  obtained at the final iteration.

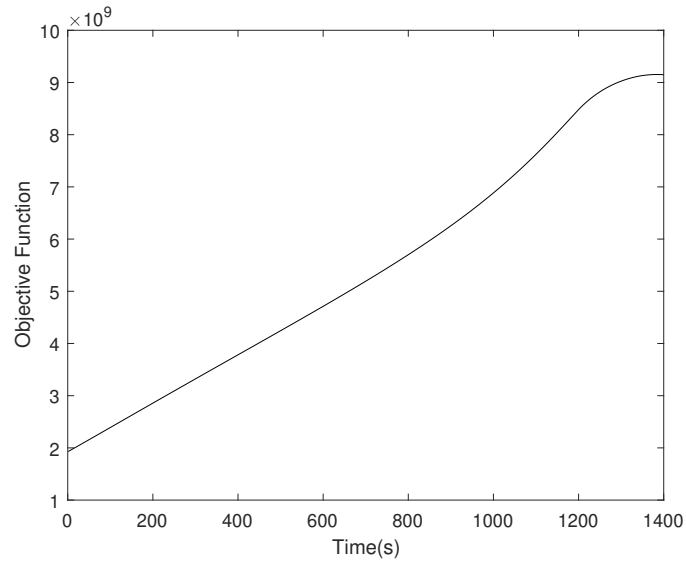


Figure 2. Objective Function  $(\mu_3^s(t) - \mu_3^n(t))$

#### 4. Optimal Control using Uncertainty Quantification

The kinetic parameters used in the Section 3 are empirical constants which are obtained through experimentation and hence, are a source of errors into the model. The exact values of the parameters are unknown and thus are termed as uncertainties which go on to produce sub-optimal results when used in real-world applications. In the next section, we convert the deterministic problem into a stochastic one, wherein the kinetic constants are treated as

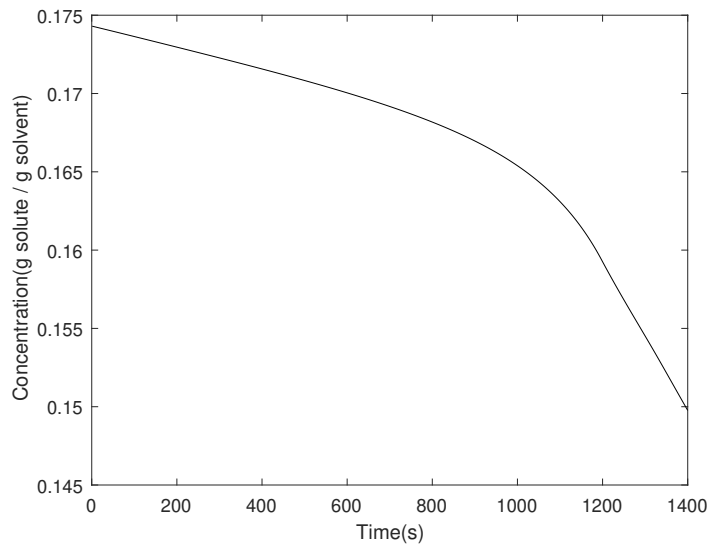


Figure 3. Concentration profile

random variables to include variation in their values into the final output produced by the model. Thus, two methods are analysed to address the given problem.

#### 4.1. Stochastic Optimal Control using Ito Processes

Several previous works have shown that the dynamic uncertainties present in batch reactors (Benavides and Diwekar (2012)) and batch distillations (Diwekar (2008)), can be represented using stochastic processes known as Ito processes. We characterize the time-dependent uncertainties in the state variables using Ito processes known as Brownian motion with drift (Diwekar (2008); Eugene and Moshe (1965)). The advantage lies in the ability to integrate the equations through the principles of stochastic calculus and the use of stochastic maximum principle to solve for the optimal temperature profile. A simple Ito process can be written as (38)

$$dy = a(y, t)dt + b(y, t)dz \quad (38)$$

where  $dz$  is the increment of the Wiener process equal to  $\varepsilon_t(\Delta t)^{1/2}$ , and  $a(y, t)$  and  $b(y, t)$  are known functions. The random value  $\varepsilon_t$  has a unit normal distribution with zero mean and a standard deviation of 1. To estimate the values of the functions  $a$  and  $b$ , a generalized method presented by Diwekar (2008) has been used.

In this work, (38) is used to modify the deterministic state (Equations (18) to (26)) to incorporate the uncertainties



into the moment equations as follows :

$$dy_1 = (-3\rho k_v G(t)(y_4 + y_8)) \Delta t + g_1 \varepsilon_1 \sqrt{\Delta t} \quad (39)$$

$$dy_2 = 0 \quad (40)$$

$$dy_3 = (G(t)y_2)\Delta t + g_3 \varepsilon_3 \sqrt{\Delta t} \quad (41)$$

$$dy_4 = (2G(t)y_3)\Delta t + g_4 \varepsilon_4 \sqrt{\Delta t} \quad (42)$$

$$dy_5 = (3G(t)y_4)\Delta t + g_5 \varepsilon_5 \sqrt{\Delta t} \quad (43)$$

$$dy_6 = (B(t))\Delta t + g_6 \varepsilon_6 \sqrt{\Delta t} \quad (44)$$

$$dy_7 = (G(t)y_6)\Delta t + g_7 \varepsilon_7 \sqrt{\Delta t} \quad (45)$$

$$dy_8 = (2G(t)y_7)\Delta t + g_8 \varepsilon_8 \sqrt{\Delta t} \quad (46)$$

$$dy_9 = (3G(t)y_8)\Delta t + g_9 \varepsilon_9 \sqrt{\Delta t} \quad (47)$$

$a(y, t)$  in each equation is replaced by the corresponding deterministic function for the state variable. Here, the  $g_i$  values represent the variance in the variable for which they are associated. They are calculated by recording the variance of the differences  $(y_i^t - y_i^{t-1})$ , which is divided by the time interval  $\Delta t$ , and then the square root of this value is taken.

The stochastic system defined by the Equations (39) to (47) treats the kinetic parameters as random variables for which the variations are propagated through the coefficients  $g_i$  into the final output of the model. The range of values exhibited by the kinetic constants can be seen in the Table 2 (Hu et al. (2005), Shi et al. (2006) and Paengjuntuek et al. (2008)). We use a Gaussian probabilistic distribution (Yenkie and Diwekar (2012)) to incorporate the variations into the model. Consequently, the objective function is also modified in (48) for its evaluation in the stochastic domain.

$$\max_T L = \mathbf{E} [\mu_3^s(t_f) - \mu_3^n(t_f)] \quad (48)$$

Here,  $\mathbf{E}$  is the expected value of the variable. The new objective function maximizes the expected value of mass of the seeded crystals for an optimal temperature profile in presence of errors or uncertainties in values of concentration or the moments, thus making it more suited to real world scenarios. The **Active Constraints** and **Initial Conditions** remain the same as mentioned in Section 3.

Table 2. Uncertainties in Kinetic Parameters

Parameters	Experimental Values	Range of Values
Growth Kinetics		
$k_g$	$1.44 \times 10^8 \mu\text{ms}^{-1}$	$1.368 - 1.512 \times 10^8$
$E_g/R$	$4859K$	$4606.15 - 5101.95$
$g$	$1.5$	$1.425 - 1.575$
Nucleation Kinetics		
$k_b$	$285(s\mu\text{m}^3)^{-1}$	$270.75 - 299.25$
$E_b/R$	$7517K$	$7141.15 - 7892.85$
$b$	$1.45$	$1.3775 - 1.5225$

#### 4.1.1. Solution Technique

The optimization problem for the given system is solved by extending the maximum principle to the Stochastic Maximum Principle (Rico-Ramirez and Diwekar (2004)), through the Steepest Ascent Hamiltonian method similar to Section 3.2. Consequently, the Hamiltonian for this section is modified to incorporate the uncertainties as :

$$H = \sum_{i=1}^9 \left( z_i F_i + \omega_i \frac{g_{y_i}^2}{2} \right) \quad (49)$$

Here,  $F_i$  are the expressions, used on the R.H.S in Equations (18) to (26). The stochastic optimal control problem has been solved in a manner similar to the deterministic problem in Section 3.2 with changes in the state Equations (39) to (47), objective function (48), Hamiltonian (49) and the number of adjoint variables. The adjoint equation formulas for the stochastic formulation are shown below in (50) and (51) (Yenkie and Diwekar (2012)). The initial and the final conditions for the variables  $y_i$  and  $z_i$  remain the same respectively whereas  $\omega_i$ 's are integrated in the backward direction using  $\omega_i(t_f) = [0 \ 0 \ 0 \ 0 \ 0 \ 0 \ 0 \ 0 \ 0]$

$$\frac{dz_j}{dt} = \sum_{i=1}^9 \left[ -\frac{\partial F_i}{\partial y_j} z_i - \frac{1}{2} \left( \frac{\partial g_i^2}{\partial y_j} \right) \omega_i \right] \quad (50)$$

$$\frac{d\omega_j}{dt} = \sum_{i=1}^9 \left[ -2\omega_i \frac{\partial F_i}{\partial y_j} - z_i \frac{\partial^2 F_i}{\partial y_j^2} - \frac{1}{2} \omega_i \left( \frac{\partial^2 g_i^2}{\partial y_j^2} \right) \right] \quad (51)$$

The algorithm followed has explained in detail below.

1. An initial temperature  $T(t) = 323K$  is assumed for the entire time horizon with  $\Delta t = 1s$ .
2. The differential equations for state variables,  $y_i$  are integrated in the forward direction at each of the above time points.
3. The values of the adjoint variables  $z_i$  and  $\omega_i$  are computed by backward integration of the adjoint differential equations.
4. Corresponding to each state and adjoint variable an addition variable is introduced to compute the hamiltonian derivative (Benavides and Diwekar (2012)).

$$\theta_i = \frac{dy_i}{dT} \quad \phi_i = \frac{dz_i}{dT} \quad \psi_i = \frac{d\omega_i}{dT} \quad (52)$$

5. Computation of  $\theta_i$  and  $\phi_i$  is done using the differential equations from (33) and (34) with the same initial and final conditions as the deterministic case, similarly the values for  $\psi_i$  are calculated using the equations obtained by (53).

$$\frac{d\left(\frac{d\omega_i}{dt}\right)}{dT} = \frac{d\left(\frac{d\omega_i}{dT}\right)}{dt} = \frac{d\psi_i}{dt} \quad (53)$$

The equations are integrated in the backward direction using the final conditions as

$$\psi_i(t_f) = [0 \ 0 \ 0 \ 0 \ 0 \ 0 \ 0 \ 0 \ 0]$$

6. The Hamiltonian derivative is now calculated at each time point as:

$$\frac{dH}{dT} = \sum_{i=1}^9 \left( \frac{dH}{dy_i} \right) \left( \frac{dy_i}{dT} \right) + \sum_{i=1}^9 \left( \frac{dH}{dz_i} \right) \left( \frac{dz_i}{dT} \right) + \sum_{i=1}^9 \left( \frac{dH}{d\omega_i} \right) \left( \frac{d\omega_i}{dT} \right) \quad (54)$$

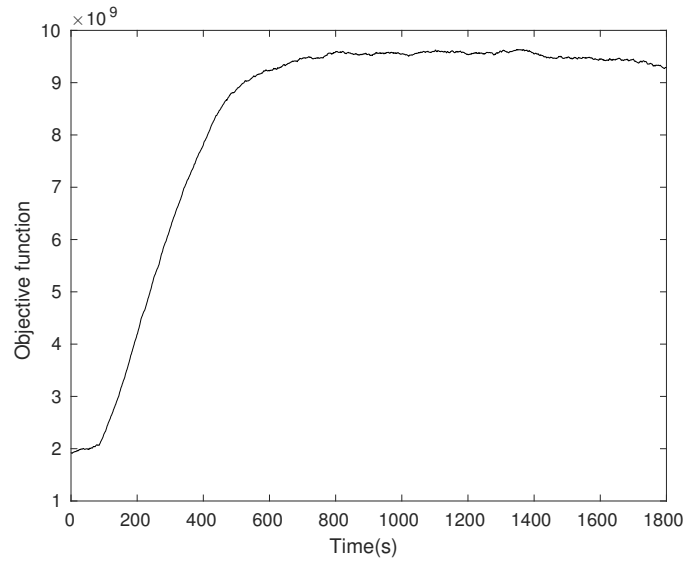
7. The computed value of the derivative is checked against the convergence criterion ( $\frac{dH}{dT} < \text{tolerance}$ ). If it is not satisfied, the temperature  $T(t)$  is updated using (37). This ensures that the optimal control variable  $T(t)$  is obtained using the extremum of Hamiltonian.
8. The concentration is evaluated at that time step and compared with first with the saturation concentration ( $C_s$ ) and then the metastable concentration ( $C_m$ ) to validate the active constraints. If it found to be lesser than saturation value or greater than the metastable value, (5) and (6) are used to compute the new temperature respectively.
9. Iterations of above steps are repeated until the convergence criteria is achieved.

#### 4.1.2. Results

The stochastic differential equations are integrated using stochastic calculus through **SDE Tools** Library available in **Matlab**. A strong Taylor approximation from the **Euler Maruyama** scheme has been used to integrate the equations which has an order of convergence of 0.5. Table 3 contains the values for  $g_i$  that were used as the coefficients for uncertainties for the state variables. In this case, the system reaches to a maximum value of the objective function at  $\sim 800s$  as seen in Figure 4. The obtained temperature profile is decreased to 309K at the end of batch time in Figure 5.

Table 3. Uncertainty Coefficients for state variables

Parameters	Values
$g_1$	$2.659 \times 10^{-5}$
$g_2$	0
$g_3$	25.882
$g_4$	$1.517 \times 10^4$
$g_5$	$6.57 \times 10^6$
$g_6$	0.5486
$g_7$	25.9
$g_8$	1382.34
$g_9$	$8.753 \times 10^4$

Figure 4. Objective Function  $[\mathbb{E}(\mu_3^s(t) - \mu_3^d(t))]$ 

#### 4.2. Stochastic Optimal Control using Polynomial Chaos Expansions

Polynomial Chaos (PC) expansions (Wiener (1938)) have risen as efficient means of representing stochastic processes with the intention of quantifying uncertainty in differential equations. PC expansions are based on a probabilistic framework and represent stochastic quantities as spectral expansions of orthogonal polynomials. In the following work, we propose the use of PC expansions to propagate uncertainty into the crystallization model and then we compare its performance with the other methods in this domain.

##### 4.2.1. Mathematical Background

The PC expansion can be considered as a mathematical model that is able to solve stochastic problems: the response of a system under stochastic effects which can be represented via a properly constructed basis functions. A stochastic process  $Y(x, t, \xi)$  with finite second-order moments and normalized random variables collected in the vector  $\xi$  can be represented as follows :

$$Y(x, t, \xi) = \mathcal{L}(x, t, \xi) \quad (55)$$

where  $t \in [0, T]$  represents the time,  $x$  is the state vector, and  $\mathcal{L}$  is an operator (linear or non-linear). Now,  $Y$  can be expressed as an infinite series of orthogonal basis functions (Ghanem and Spanos (1990), Ghanem and Spanos (1997)),

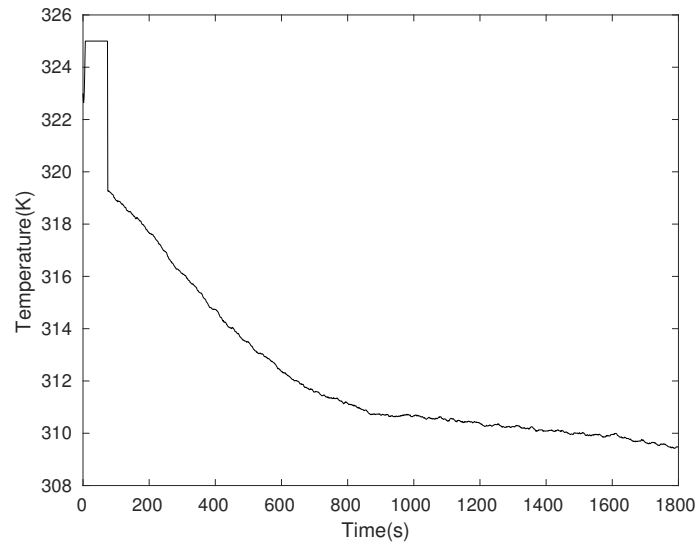
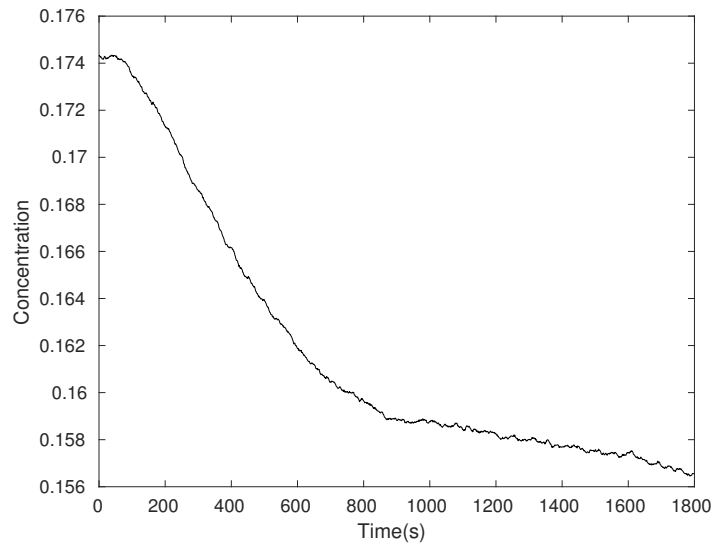
Figure 5. The optimal cooling profile  $T(t)$  obtained for the system

Figure 6. Concentration Profile

$\Phi_i$  with suitable deterministic coefficients  $a_i$  as :

$$Y(t, \xi) = \sum_{i=0}^{\infty} a_i(t) \Phi_i(\xi) \quad (56)$$

where the representation in (56) is exact. However, for practical applications, Equation (56) is truncated to a limited number of basis functions  $M + 1$  and is represented as :

$$Y(t, \xi) \approx \sum_{i=0}^M a_i(t) \Phi_i(\xi) \quad (57)$$

The total number of terms depends on the number of dimensions,  $N$  of the random multivariate parameter  $\xi$  and the highest order  $P$  of the polynomials  $\Phi_i$  which is set according to the required accuracy. The number of terms now become  $M + 1 = \frac{(N+P)!}{N!P!}$ . The basis functions  $\Phi_i$  used for generating polynomial expansions are chosen from the Askey scheme (Xiu and Karniadakis (2002)) which maps the polynomial functions to the type of stochastic distribution of the random variables( $\xi$ ) that are considered in the model. In our case, the parameters follow a Gaussian distribution (Yenkie and Diwekar (2012)), which uses Hermite Polynomials to describe the probability distribution in the least number of terms. In particular, if the random variables  $\xi$  are independent, their joint probability distribution function (PDF) corresponds to the product of the distributions of each random variable.

Given a process model with uncertain output,  $y = f(x, \lambda)$ , where  $x$  is the uncertain input and  $\lambda$  is the uncertain parameter, the aim is to quantify uncertainty in  $y(\xi)$  from  $x(\xi)$  and  $\lambda(\xi)$  by representing each of these variables as a polynomial expansion of basis functions. The crystallization model given by Equations (29) to (31) corresponds to these notations as follows.  $\lambda$  is the set of kinetic parameters given in Table 3 whereas  $\xi$  is a random variable of the Gaussian distribution. The first step is to construct PCE's of  $x(\xi)$ , and  $\lambda(\xi)$ , by determining their PCE coefficients  $x_i$  and  $\lambda_i$  where (59) utilises the orthogonality condition of the basis functions.

$$x(\xi) = \sum_{i=0}^M x_i \phi_i(\xi) \quad \lambda(\xi) = \sum_{i=0}^M \lambda_i \phi_i(\xi) \quad (58)$$

$$x_i = \frac{\int x \phi_i(\xi) g(\xi) d\xi}{\langle \phi_i^2 \rangle} \quad \lambda_i = \frac{\int \lambda \phi_i(\xi) g(\xi) d\xi}{\langle \phi_i^2 \rangle} \quad (59)$$

Here  $g(\xi)$  is PDF of  $\xi$ . The next step is to develop PCE for  $y(\xi)$  which can be done by evaluating the inner product of  $y(\xi)$  with each of the basis functions  $\phi_i$  to determine the  $i$ th- PCE coefficient as follows.

$$y_i = \frac{\langle f(x, \lambda) \phi_i \rangle}{\langle \phi_i^2 \rangle} \quad (60)$$

Evaluating the inner product  $\langle y \phi_i \rangle$ , requires computation of multi-dimensional integrals which can be performed by one of two approaches referred to as **non-intrusive** and **intrusive**. The first are sampling-based methods requiring to solve the problem at hand multiple times for specific values of the random variables considered, chosen according to a suitable sampling strategy (Xiu (2010)). A deterministic problem is solved at each iteration. This strategy is similar to MC-based methods, with the important difference that the number of samples required for the computation of PC models is limited. The latter requires modification of the fundamental equations governing the system under study in order to obtain a new system of equations where the desired PC coefficients are the unknowns (Eldred (2009)). The main difference between these two approaches is that non-intrusive techniques are easy to implement and use existing deterministic model (Section 2) as black-box(no modifications of the system fundamental equations are required), while intrusive ones generally lead to a coupled system of equations, which can be more expensive to solve with respect to the original problem. Thus, this paper uses the non-intrusive approach to solve for the PC coefficients. The detailed approach has been explained in the following sections.

#### 4.2.2. Usage of PCE in Batch Crystallization

Application of the polynomial chaos methodology (Streif et al. (2014)) to seeded batch crystallization requires identifying the corresponding parameters mentioned in Section 4.2.1. The state variables  $y_i$  (Equations (18) to (26)) act as the uncertain outputs  $Y$ , caused by uncertainties present in process parameters  $\lambda$  ( $k_g, E_g, g, k_b, E_b, b$ ), that are used to calculate the Growth rate (4) and the Nucleation rate (62). Temperature( $T(t)$ ) acts as the input variable  $x$  in

the system. Here,  $\xi$  represents the joint distribution of the random variables which are modelled using the Gaussian probabilistic distribution (Yenkie and Diwekar (2012)).

The PC expansion coefficients are determined using the probabilistic collocation method (Mesbah et al. (2014), Nagy and Braatz (2007)), a non-intrusive approach in which  $N$  samples are drawn from the known distributions of uncertainties and, subsequently, are used to solve the non-linear process model. This approach proves beneficial as the deterministic model implemented previously in is utilised here as an application to compute the process outputs. The PC expansion coefficients are now obtained in a least squares sense by minimizing the residuals between the PC expansion and the non-linear model predictions. The complete algorithm is discussed below.

1. A joint probability distribution is constructed by combining the individual uncertain parameters  $[k_g, E_g, g, k_b, E_b, b]$ , each of which is modelled using a Gaussian distribution.
2. Through experimentation, order of the polynomials was fixed at  $P = 2$  as the resulting PC expansion was able to achieve sufficient accuracy. The number of terms was derived as given in Section 4.2.1. This determined the collocation points at which the model is simulated.
3. Samples are generated for the model at  $N$  collocation points. The sampling technique used is the Gaussian Quadratures along with Hermite Polynomials to represent state variables  $y_i$  in the form of (57).
4. The deterministic algorithm developed in Section 3 is now used to calculate the output at each of the simulation points.
5. For each of the above sample  $y_i^j = f(T^j(\xi), \lambda(\xi))$ , the optimization problem is solved using the Steepest Ascent Hamiltonian method discussed.
6. The optimum value of the input temperature  $T^j(\xi)$  at each of these samples is used to construct the PC expansion for  $T(\xi)$  and  $\lambda(\xi)$  (58 and 59), by using the orthogonal property of the basis functions.
7.  $y_i^j$ 's for each sample are used to evaluate :

$$y_i = \frac{1}{\langle \phi_i^2 \rangle} \frac{1}{N} \sum_{j=1}^N y_i^j \phi_i(\xi) \quad (61)$$

Here,  $\phi_i$  are the coefficients of the orthogonal polynomials being used for PCE estimation.

8. As the above Equation averages over  $N$  samples, the resultant  $y_i$  maximises the objective function, given by  $\mathbf{E}\{y_5 - y_9\}$ .

#### 4.2.3. Results

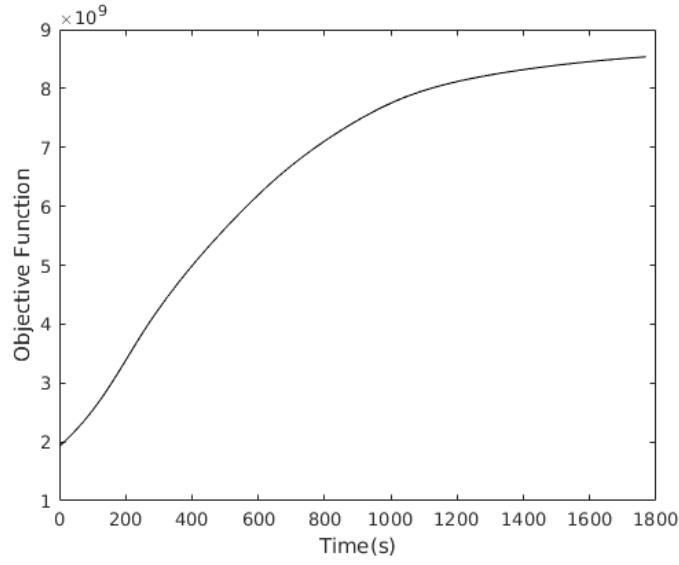
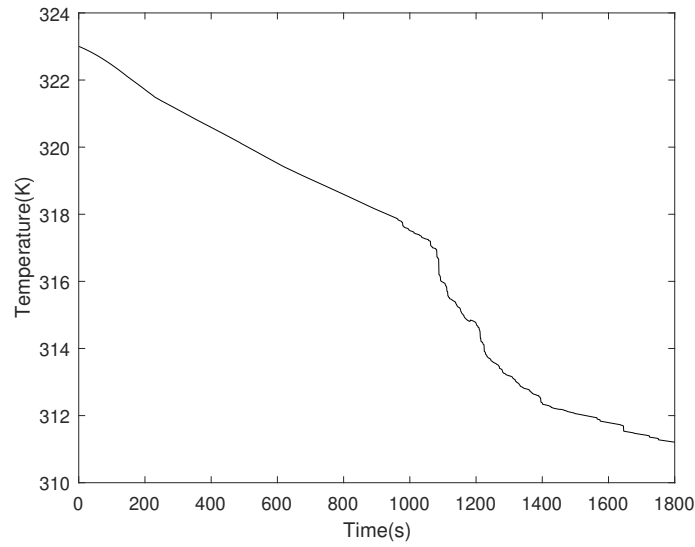
All the source scripts for using PCE with the crystallization model were written Python, using the open source library **chaospy** (Feinberg and Langtangen (2015)). It is a toolbox for performing uncertainty quantification through polynomial chaos expansions and efficient sampling strategies. The base model for performing simulations was derived from Section 3. The range of values exhibited by the uncertain parameters have been mentioned in the Table 2. The results obtained can be observed from Figures 7, 8 and 9.

## 5. Case Study

In the following study, the insights gathered from our work on batch seeded crystallization has been extended to the unseeded batch cooling crystallization of L-Asparagine Monohydrate (LAM) to develop a predictive model based on a population balance framework and at the same time validate the performance of the Polynomial Chaos (PC) approach in this domain. Similar to the previous sections, we aim to predict an optimal cooling strategy to achieve a desired objective function value.

### 5.1. Mathematical Background

Previous works in literature have reported the determination of nucleation and growth kinetic parameters of LAM during anti-solvent crystallization at high supersaturation (Lindenberg and Mazzotti (2011), Mahajan and Kirwan (1994) and Zarkadas and Sirkar (2006)). Also, Bhoi et al. (2017) published a non-linear approach on kinetic parameter estimation using experimental data which has been utilized further in this study.

Figure 7. Objective Function  $[E(\mu_3^s(t) - \mu_3^n(t))]$ Figure 8. The optimal cooling profile  $T(t)$  obtained for the system

The formation of LAM crystals are modelled using the population balance equation in (2), whereas the nucleation and the growth rate expressions are modified to incorporate the differences in kinetics from the previous model. The rate of formation on nuclei is given by (62) (Lindenberg and Mazzotti (2011)),

$$B = k_{j_1} S \exp\left(-k_{j_2} \frac{\ln^3 C_c / C^*}{\ln^2 S}\right) \quad (62)$$

in which  $C_c$  represents the molar density of LAM crystals. Here,  $k_{j_1}$  and  $k_{j_2}$  are empirical parameters. The growth

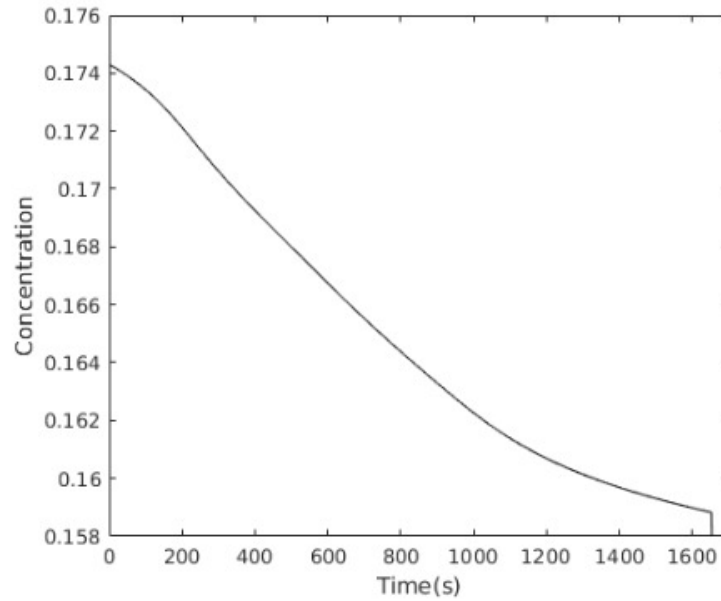


Figure 9. Concentration profile

rate (Nagy and Braatz (2007) and Nagy et al. (2008)) is now given by the power-law expression in (63).

$$G = k_g(S - 1)^g \quad (63)$$

The supersaturation ratio,  $S$ , is defined as :

$$S = C/C^* \quad (64)$$

where  $C^*$  represents the saturation concentration of LAM crystals. The solubility of these crystals can be expressed as:

$$C^* = 5 \times 10^{-5}T^2 - 0.001T + 0.0236 \quad (65)$$

Bhoi et al. (2017) used a predictive non-linear technique which minimizes the difference between the experimental and predicted concentrations of LAM crystals to estimate the values of the set of kinetic parameters  $[k_g, g, k_{j1}, k_{j2}]$ . Table 4 depicts the resulting values.

Similar to the procedure followed in Section 2, Method of Moments has been used to reduce the PBE to ODE's given by Equations (66) to (67). The mass balance for LAM crystals also remains the same, with the difference being the absence of seeded crystals.

$$\frac{du_0}{dt} = B \quad (66)$$

$$\frac{du_j}{dt} = jG\mu_{j-1} \quad \text{for } j = 1, 2, 3, 4 \quad (67)$$

Determination of the optimal temperature profile for maximizing the weight mean size of crystals is a very common objective for a crystallization process (Mao et al. (2010), Nowee et al. (2007) and Yang and Nagy (2013)). The current process is an unseeded batch process as compared to the previous seeded one, thus the following optimal control problem is formulated. The **Objective Function** becomes :

$$\max_{T(t)} \phi = \mu_4/\mu_3 \quad \text{at } t = t_f \quad (68)$$



which is subject to the **Constraints** :

$$T_{min} \leq T(t) \leq T_{max} \quad (69)$$

$$\frac{dT}{dt} \leq 0 \quad (70)$$

The state variables can be represented as :

$$y_i = [ \quad C \quad \mu_0 \quad \mu_1 \quad \mu_2 \quad \mu_3 \quad \mu_4 \quad ]$$

Table 4. Estimated values for kinetic parameters

Parameters	Experimental Values	Range of Values
Growth Kinetics		
$\ln(k_g)$	$3.41 \pm 0.28$	$\mu m min^{-1}$
$g$	$1.48 \pm 0.04$	–
Nucleation Kinetics		
$\ln(k_{j_1})$	$24.74 \pm 0.73$	$No. perm^3 min$
$k_{j_2}$	$2.7 \times 10^{-2} \pm 3.2 \times 10^{-3}$	–

### 5.2. Solution Technique : Hamiltonian Steepest Ascent with PCE

Solution to the unseeded crystallization scenario involved application of the PCE technique described in Section 4.2. The Hamiltonian method was employed to solve the optimization problem. Equations (66) to (67) take place as the new state equations and the uncertain parameters are mentioned in Table 4. The constraint equation (69) depicts a cooling strategy for the crystallizer. The objective function here (68) calculates the final maximum mean size of the crystals.

The key differences in the problem from the one used in previous sections.

- The crystallization does not involve the presence of initial seeded crystals and thus does not involve 2 separate types of moments.
- The batch time for the model was taken to be 240 min( $t_f$ ).
- An initial concentration value of 0.073 g/L was taken to obtain the cooling profile. All the moments were initialised to 0.

### 5.3. Results

The ODEs were integrated using Python **scipy's odeint** integrator. The concentration profile and the cooling trajectory for the time horizon can be seen in Figure 10 and 11. These results produced the following insights :

- The final value of the objective function( $\mu_4/\mu_3$ ), ie. the mean crystal size was obtained at :  $300\mu m$
- The model performs at par with other cooling policies such as the cubic cooling policy,  $251\mu m$  (Bhoi et al. (2017)). This proves the efficacy of polynomial chaos expansions in the field of batch crystallization.

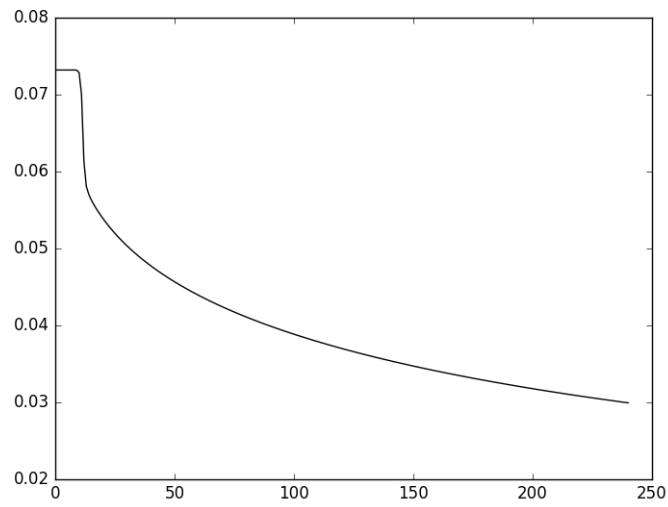


Figure 10. Concentration Profile

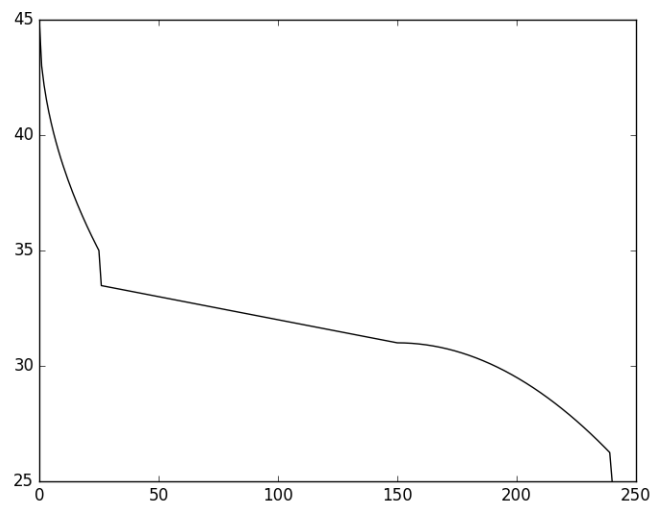


Figure 11. Temperature Profile

## 6. Conclusion

- The same process was optimized using 3 different methods of Optimization with the aim maximising the volume of the product obtained.
- The Temperature profile for all the 3 cases was obtained as a decreasing one and thus follows the principle of batch cooling crystallization.
- Polynomial Chaos Expansions, when applied to crystallization performs at par with the existing methods in

optimizing the process by efficiently incorporating uncertainties.

- After comparing the final values of the objective functions( $\mu_3^s - \mu_3^n$ )[particle volume] the following values were obtained :
  1. Deterministic :  $9.153 \times 10^9 \mu m^3$
  2. Expected value for Stochastic involving Ito Processes :  $9.2 \times 10^9 \mu m^3$
  3. Expected value for Stochastic case involving PCE :  $8.64 \times 10^9 \mu m^3$
- The decrease of values can be attributed to the presence of errors or uncertainties in the kinetic parameters. Thus, the model becomes helpful in predicting the expected values for volume of crystals taking care of the process uncertainties.

## References

- Benavides, P. T. and Diwekar, U. (2012). Optimal control of biodiesel production in a batch reactor: Part ii: Stochastic control. *Fuel*, 94:218–226.
- Bhoi, S., Lenka, M., and Sarkar, D. (2017). Particle engineering by optimization for the unseeded batch cooling crystallization of l-asparagine monohydrate. *CrystEngComm*, 19(42):6373–6382.
- Corriou, J.-P. and Rohani, S. (2008). A new look at optimal control of a batch crystallizer. *AIChE journal*, 54(12):3188–3206.
- Diwekar, U. (2008). *Introduction to applied optimization*, volume 22. Springer Science & Business Media.
- Eldred, M. (2009). Recent advances in non-intrusive polynomial chaos and stochastic collocation methods for uncertainty analysis and design. page 2274.
- Eugene, W. and Moshe, Z. (1965). On the relation between ordinary and stochastic differential equations. *International Journal of Engineering Science*, 3(2):213–229.
- Feinberg, J. and Langtangen, H. P. (2015). Chaospy: An open source tool for designing methods of uncertainty quantification. *Journal of Computational Science*, 11:46–57.
- Ghanem, R. and Spanos, P. D. (1990). Polynomial chaos in stochastic finite elements. *Journal of Applied Mechanics*, 57(1):197–202.
- Ghanem, R. G. and Spanos, P. D. (1997). Spectral techniques for stochastic finite elements. *Archives of Computational Methods in Engineering*, 4(1):63–100.
- Grosso, M., Cogoni, G., Baratti, R., and Romagnoli, J. A. (2011). Stochastic approach for the prediction of psd in crystallization processes: Formulation and comparative assessment of different stochastic models. *Industrial & Engineering Chemistry Research*, 50(4):2133–2143.
- Hu, Q., Rohani, S., and Jutan, A. (2005). Modelling and optimization of seeded batch crystallizers. *Computers & chemical engineering*, 29(4):911–918.
- Jones, A. (1974). Optimal operation of a batch cooling crystallizer. *Chemical Engineering Science*, 29(5):1075–1087.
- Kim, K. K. K. and Braatz, R. D. (2012). Probabilistic analysis and control of uncertain dynamic systems: Generalized polynomial chaos expansion approaches. pages 44–49.
- Kumar, D. and Budman, H. (2014). Robust nonlinear mpc based on volterra series and polynomial chaos expansions. *Journal of Process Control*, 24(1):304–317.
- Lindenberg, C. and Mazzotti, M. (2011). Continuous precipitation of l-asparagine monohydrate in a micromixer: Estimation of nucleation and growth kinetics. *AIChE journal*, 57(4):942–950.
- Ma, D. L., Chung, S. H., and Braatz, R. D. (1999). Worst-case performance analysis of optimal batch control trajectories. *AIChE journal*, 45(7):1469–1476.
- Mahajan, A. J. and Kirwan, D. J. (1994). Nucleation and growth kinetics of biochemicals measured at high supersaturations. *Journal of crystal growth*, 144(3–4):281–290.
- Mao, S., Zhang, Y., Rohani, S., and Ray, A. K. (2010). Kinetics of (r, s)- and (r)-mandelic acid in an unseeded cooling batch crystallizer. *Journal of Crystal Growth*, 312(22):3340–3348.
- Mesbah, A., Streif, S., Findeisen, R., and Braatz, R. D. (2014). Active fault diagnosis for nonlinear systems with probabilistic uncertainties. *IFAC Proceedings Volumes*, 47(3):7079–7084.
- Miller, S. M. and Rawlings, J. B. (1994). Model identification and control strategies for batch cooling crystallizers. *AIChE Journal*, 40(8):1312–1327.
- Mullin, J. and Nývlt, J. (1971). Programmed cooling of batch crystallizers. *Chemical Engineering Science*, 26(3):369–377.
- Nagy, Z. and Braatz, R. (2007). Distributional uncertainty analysis using power series and polynomial chaos expansions. *Journal of Process Control*, 17(3):229–240.
- Nagy, Z. K., Fujiwara, M., Woo, X. Y., and Braatz, R. D. (2008). Determination of the kinetic parameters for the crystallization of paracetamol from water using metastable zone width experiments. *Industrial & Engineering Chemistry Research*, 47(4):1245–1252.
- Nowee, S. M., Abbas, A., and Romagnoli, J. A. (2007). Optimization in seeded cooling crystallization: A parameter estimation and dynamic optimization study. *Chemical Engineering and Processing: Process Intensification*, 46(11):1096–1106.
- Paengjuntuek, W., Arpornwichanop, A., and Kittisupakorn, P. (2008). Product quality improvement of batch crystallizers by a batch-to-batch optimization and nonlinear control approach. *Chemical Engineering Journal*, 139(2):344–350.
- Rawlings, J. B., Witkowski, W. R., and Eaton, J. W. (1992). Modelling and control of crystallizers. *Powder technology*, 69(1):3–9.
- Rico-Ramirez, V. and Diwekar, U. M. (2004). Stochastic maximum principle for optimal control under uncertainty. *Computers & Chemical Engineering*, 28(12):2845–2849.
- Shi, D., El-Farra, N. H., Li, M., Mhaskar, P., and Christofides, P. D. (2006). Predictive control of particle size distribution in particulate processes. *Chemical Engineering Science*, 61(1):268–281.
- Streif, S., Karl, M., and Mesbah, A. (2014). Stochastic nonlinear model predictive control with efficient sample approximation of chance constraints. *arXiv preprint arXiv:1410.4535*.
- Wiener, N. (1938). The homogeneous chaos. *American Journal of Mathematics*, 60(4):897–936.
- Xiu, D. (2010). Numerical methods for stochastic computations: a spectral method approach.
- Xiu, D. and Karniadakis, G. E. (2002). The wiener–askey polynomial chaos for stochastic differential equations. *SIAM journal on scientific computing*, 24(2):619–644.
- Yang, Y. and Nagy, Z. K. (2013). Model-based systematic design and analysis approach for unseeded combined cooling and antisolvent crystallization (ccac) systems. *Crystal Growth & Design*, 14(2):687–698.
- Yenkie, K. M. and Diwekar, U. (2012). Stochastic optimal control of seeded batch crystallizer applying the ito process. *Industrial & Engineering Chemistry Research*, 52(1):108–122.
- Zarkadas, D. M. and Sirkar, K. K. (2006). Antisolvent crystallization in porous hollow fiber devices. *Chemical engineering science*, 61(15):5030–5048.